Side Moment Exerted by a Two-Component Liquid Payload on a Spinning Projectile

Charles H. Murphy*
U.S. Army Laboratory Command, Ballistic Research Laboratory, Aberdeen Proving Ground, Maryland

A linear boundary layer theory for two liquids in a cylindrical cavity in a coning and spinning projectile is derived. Predicted eigenfrequencies agree well with available experimental results. Side moment coefficients are computed for various cases. It is shown that significant increases in the single-liquid side moment can be caused by the addition of a small amount of heavier liquid, and for certain locations of the liquid interface, pairs of eigenfrequencies can coalesce. Good agreement between predicted side moment and recently measured side moment is also shown.

Nomenclature

a = radius of the cylindrical cavity containing the liquids
b_1 = radius of the interface of the two liquids for $K_1 = 0$
b_2 = radius of an air core (or central rod) for $K_1 = 0$
c = half-height of the cylindrical cavity containing the liquids
C_{LIM} = liquid in-plane moment coefficient
C_{LSM} = liquid side moment coefficient
f = $1-(b_2/a)^2$, the fill ratio
$\hat{K}$ = $K_1(0)e^{i\phi_1(0)}$
$K_1(t)$ = amplitude of the coning motion
m_L = $2\pi\rho_1 a^2 c$, the liquid mass in the cavity fully filled with liquid 1
$M_{L\tilde{Y}}, M_{L\tilde{Z}}$ = $\tilde{Y}$, $\tilde{Z}$ components of the liquid moment
N = $\rho_{21}(\nu_2/\nu_2)^{1/2}$
N_k = number of terms considered in summing for $k = 1,3,5,\ldots\ (2N_k - 1)$
P = liquid pressure
p_j = pressure perturbation in liquid j
p_{ji} = inviscid part of p_j
$\tilde{p}_{ji}$ = $p_{ji} - (\tilde{r}\tilde{x}/a^2)\tilde{K}$
p_{jv} = viscous part of p_j
r = radial coordinate in the inertial system
$\tilde{r}$ = radial coordinate in the aeroballistic system
Re{ } = real part of { }
Re_j = $a^2\dot{\phi}\nu_j^{-1}$, Reynolds number for liquid j
s = $(\epsilon + i)\tau$
S = $s^2 - 2is + 3$
s_{kn} = eigenvalues of s: the values of s that make the determinant of the least squares equations for Eq. (56) zero
t = time
u_j, v_j, w_j = x, r, θ components of the liquid j velocity perturbation
u_{ji}, v_{ji}, w_{ji} = inviscid part of u_j, v_j, w_j
u_{jv}, v_{jv}, w_{jv} = viscous part of u_j, v_j, w_j
$V_{xj}, V_{rj}, V_{\theta j}$ = x, r, θ components of the liquid j velocity
x = axial coordinate in the inertial system
$\tilde{x}$ = axial coordinate in the aeroballistic system
XYZ = inertial Cartesian axes, the X-axis tangent to the trajectory at time zero
$\tilde{X}\tilde{Y}\tilde{Z}$ = aeroballistic system Cartesian axes, the $\tilde{X}$ axis along the missile's axis of symmetry
$\tilde{\alpha}$ = angle of attack: the projection in the $\tilde{X}\tilde{Z}$ plane of the angle between the X and $\tilde{X}$ axes
$\tilde{\beta}$ = angle of sideslip: the projection in the $\tilde{X}\tilde{Y}$ plane of the angle between the X and $\tilde{X}$ axes
δ_{aj} = complex radial displacement thickness
δ_{cj} = complex axial displacement thickness
Δp_i = fluctuating part of the inviscid pressure
ϵ = $(\dot{K}_1/K_1)\dot{\phi}_1^{-1}$, nondimensionalized damping
ϵ_1 = $\exp[(b_1 - a)/a\delta_{a1}]$
ϵ_2 = $\exp[(b_2 - b_1)/a\delta_{a2}]$
η_j = dimensionless perturbation of liquid interfaces due to coning motion
θ = azimuthal coordinate in the inertial system
$\tilde{\theta}$ = azimuthal coordinate in the aeroballistic system
λ_k = "average" value of λ_{jk}
λ_{jk} = $(\pi k/2)(1 + \delta_{cj})$
$\bar{\lambda}_{jk}$ = $[S^{1/2}/(1+is)]\lambda_{jk}$
μ_j = $\nu_j\rho_j$, dynamic viscosity of liquid j
ν_j = kinematic viscosity of liquid j
ρ_j = density of liquid j
ρ_{21} = density ratio, $\rho_2/\rho_1 \le 1$
τ = $\dot{\phi}_1/\dot{\phi}$, nondimensionalized frequency
τ_{kn} = eigenfrequency for modes k and n; the imaginary part of s_{kn}
ϕ = dimensionless time, $\dot{\phi}t$
$\dot{\phi}$ = spin rate relative to inertia axes
$\phi_1(t)$ = phase angle of the coning motion

Subscripts and Superscripts

e = endwall
j = liquid no. (1 heavier, 2 lighter)
k = axial mode no. 1, 3, 5, ...$(2N_k - 1)$
ℓ = lateral wall
n = radial mode no. 1, 2, 3,...
p = pressure component
v = viscous (wall shear) component
$(\dot{})$ = d( )/dt
$(\,)'$ = d( )/dr

Presented as Paper 84-2115 at the AIAA Atmospheric Flight Mechanics Conference, Seattle, WA, Aug. 21-23, 1984; received Dec. 5, 1984; revision received April 8, 1986.

*Chief, Launch and Flight Division. Fellow AIAA.

I. Introduction

THE ability to predict the complete moment exerted by a spinning liquid payload on a spinning and coning projectile has been a problem of considerable interest to the Army for some time. For a fully spinning liquid, the linear side moment was first computed by Stewartson[1] for an inviscid payload by use of fluid oscillation eigenfrequencies determined by the fineness ratio of the cylindrical container. Wedemeyer[2] introduced boundary layers on the walls of the container and was able to determine viscous corrections for Stewartson's eigenfrequencies, which could then be used in Stewartson's side moment calculation. Murphy[3] then completed the linear boundary layer theory by including all pressure and wall shear contributions to the liquid-induced side moment. The Stewartson-Wedemeyer eigenvalue calculations have been improved by Kitchens et al.[4] for low Reynolds numbers through the replacement of the cylindrical wall boundary approximation by a linearized Navier-Stokes (NS) approach. Next, Gerber et al.[5,6] extended this linearized NS technique to compute better side moment coefficients for Reynolds numbers less than 10,000. Finally, the roll moment for a fully spun-up liquid was computed by Murphy.[7,8]

An important limitation of this work has been the restriction to a single liquid in the payload. Scott[9] derived relations for eigenfrequencies for two inviscid liquids and obtained fair experimental agreement. For Scott's inviscid liquids, the tangential perturbation velocities have discontinuous jumps at the two-liquid interface.

In this paper we will consider two viscous liquids, although we will restrict our consideration of viscosity to boundary layers near the cylinder inner surfaces and near the two-liquid interface. The remainder of the liquid will be considered inviscid. Under these assumptions, side moment coefficents and eigenfrequencies will be computed.

II. Liquid Boundary Conditions

Two coordinate systems will be used in this paper: the nonrolling aeroballistic $\tilde{X}\tilde{Y}\tilde{Z}$ system, whose $\tilde{X}$ axis is fixed along the missile's axis of symmetry, and the inertial XYZ system, whose X axis is tangent to the trajectory at time zero. Both coordinate systems have origins at the center of the cylindrical payload cavity, which is assumed to be at the center of mass of the projectile. Location in the cavity can be specified by the cylindrical coordinates $\tilde{x}$, $\tilde{r}$, and $\tilde{\theta}$ in the aeroballistic system, and by x, r, and θ in the inertial system. The boundary of the cavity is given by $\tilde{x}=\pm c$ and $\tilde{r}=a$, where $2c$ is the height of the cavity and $2a$ is its diameter. The projectile is assumed to be performing a coning motion of amplitude $K_1(t)$ and a phase angle $\phi_1(t)$. If $\tilde{\alpha}$ and $\tilde{\beta}$ are the angles of attack and side-slip of the missile's axis with respect to the trajectory (the X axis), then

$$\tilde{\beta}+i\tilde{\alpha}=K_1e^{i\phi_1}=\hat{K}e^{s\phi} \tag{1}$$

where $\phi=\dot{\phi}t$, $s=(\epsilon+i)\tau$, $\hat{K}=K_1(0)e^{i\phi_1(0)}$, $\tau=\dot{\phi}_1/\dot{\phi}$, $\tau\epsilon\dot{\phi}=\dot{K}_1/K_1$, and $\dot{\phi}$ is the axial component of the angular velocity relative to inertia axes and is assumed to be positive and constant. Linear relations between cylindrical coordinates in the two coordinate systems were derived in Ref. 3 as

$$\tilde{x}=x-rK_1\cos(\phi_1-\theta)=x-r\mathrm{Re}\{\hat{K}e^{s\phi}\} \tag{2}$$

$$\tilde{r}=r+xK_1\cos(\phi_1-\theta)=r+x\mathrm{Re}\{\hat{K}e^{s\phi}\} \tag{3}$$

$$\tilde{\theta}=\theta+(x/r)K_1\sin(\phi_1-\theta)=\theta-(x/r)\mathrm{Re}\{i\hat{K}e^{s\phi}\} \tag{4}$$

where $\mathrm{Re}\{\ \}=[\{\ \}+\{\bar{\ }\}]/2$ is the real part of a complex quantity.

The two liquids have densities ρ_1 and ρ_2 ($\rho_1\geq\rho_2$) and kinematic viscosities ν_1 and ν_2. When the liquids are fully spun up and $K_1=0$, liquid 1 occupies the cylindrical annular region $b_1\leq r\leq a$ and liquid 2 occupies the cylindrical annular region $b_2\leq r\leq b_1$. The fill ratio f is the ratio of the volume of the annular region containing both liquids to that of the complete cylinder, i.e., $1-(b_2/a)^2$. The surface $r=b_2$ is either a free surface or the surface of a rigid central rod. The free surface boundary will be considered in this paper (the central rod is discussed in Ref. 10). For a fully filled cylinder, $b_2=0$ and $f=1$.

When the cylinder is forced to perform a coning motion, the interface between the liquids is located at

$$r_1=b_1(1+\eta_1) \tag{5}$$

where $|\eta_1(x,\theta,t)|\ll 1$ and the free inner surface is located at

$$r_2=b_2(1+\eta_2) \tag{6}$$

where $|\eta_2(x,\theta,t)|\ll 1$.

The velocity components in the two liquids have a very simple form:

$$V_{xj}=\mathrm{Re}\{u_je^{s\phi-i\theta}\}a\dot{\phi} \tag{7}$$

$$V_{rj}=\mathrm{Re}\{v_je^{s\phi-i\theta}\}a\dot{\phi} \tag{8}$$

$$V_{\theta j}=\dot{\phi}r+\mathrm{Re}\{w_je^{s\phi-i\theta}\}a\dot{\phi} \tag{9}$$

where $j=1,2$.

The fluid pressure, however, has a more complicated form:

$$\begin{aligned}
P&=P_0, \qquad 0\leq r\leq r_2\\
&=P_0+\rho_2\dot{\phi}^2\left[\frac{r^2-b_2^2}{2}\right]+\mathrm{Re}\{p_2e^{s\phi-i\theta}\}\rho_2a^2\dot{\phi}^2, \qquad r_2\leq r\leq r_1\\
&=P_0+\rho_2\dot{\phi}^2\left[\frac{b_1^2-b_2^2}{2}\right]+\rho_1\dot{\phi}^2\left[\frac{r^2-b_1^2}{2}\right]\\
&\quad+\mathrm{Re}\{p_1e^{s\phi-i\theta}\}\rho_1a^2\dot{\phi}^2, \qquad r_1\leq r\leq a
\end{aligned} \tag{10}$$

If we assume the small perturbation of the interface surface has the same form as the perturbation velocities, then

$$\eta_1=\mathrm{Re}\{\hat{\eta}_1(x)e^{s\phi-i\theta}\} \tag{11}$$

By using Eqs. (5) and (11), the equation of the interface surface is

$$F(x,r,\theta,t)=r-b_1-\mathrm{Re}\{b_1\hat{\eta}_1e^{s\phi-i\theta}\}=0 \tag{12}$$

At the interface, the two liquids have the same velocity, i.e., the velocity of the interface itself.

$$\therefore\frac{\mathrm{d}F}{\mathrm{d}t}=V_{xj}\frac{\partial F}{\partial x}+V_{rj}\frac{\partial F}{\partial r}+\frac{V_{\theta j}}{r}\frac{\partial F}{\partial\theta}+\frac{\partial F}{\partial t}=0 \tag{13}$$

When only linear terms are retained, this reduces to

$$b_1\hat{\eta}_1(x)=\frac{av_1(b_1,x)}{s-i}=\frac{av_2(b_1,x)}{s-i} \tag{14}$$

Similarly, the perturbation of the inner surface has the form

$$b_2\hat{\eta}_2(x)=\frac{av_2(b_2,x)}{s-i} \tag{15}$$

where $\eta_2=\mathrm{Re}\{\hat{\eta}_2e^{s\phi-i\theta}\}$.

In addition to three continuous velocity components at the interface, we require that the pressure and the two viscous shears are continuous at the interface. Equations (10) and (14)

yield a simple pressure relation at the interface:

$$p_1(b_1,x)+\frac{b_1 v_1(b_1,x)}{a(s-i)}=\rho_{21}\left[p_2(b_1,x)+\frac{b_1 v_2(b_1,x)}{a(s-i)}\right] \quad (16)$$

where $\rho_{21}=\rho_2/\rho_1$. If only velocity gradients normal to the interface are considered, the continuous viscous shear assumptions imply that

$$\mu_1\frac{\partial u_1(b_1,x)}{\partial r}=\mu_2\frac{\partial u_2(b_1,x)}{\partial r} \quad (17)$$

$$\mu_1\frac{\partial w_1(b_1,x)}{\partial r}=\mu_2\frac{\partial w_2(b_1,x)}{\partial r} \quad (18)$$

At the cylinder surface, the liquid must have the rigid body motion of the cylinder:

$$u_1=(s-i)\hat{K} \quad (19)$$

$$v_1=-(s-i)(x/a)\hat{K} \quad (20)$$

$$w_1=i(s-i)(x/a)\hat{K} \quad (21)$$

Finally, at the free surface, the pressure is constant and the viscous shears are zero:

$$p_2(b_2,x)+\frac{b_2 v_2(b_2,x)}{a(s-i)}=0 \quad (22)$$

$$\mu_2\frac{\partial u_2(b_2,x)}{\partial r}=0 \quad (23)$$

$$\mu_2\frac{\partial w_2(b_2,x)}{\partial r}=0 \quad (24)$$

III. The Inviscid Solution

The perturbation functions are written as sums of viscous and inviscid parts:

$$u_j=u_{ji}+u_{jv} \qquad w_j=w_{ji}+w_{jv}$$

$$v_j=v_{ji}+v_{jv} \qquad p_j=p_{ji}+p_{jv} \quad (25)$$

Table 1 Inviscid perturbation functions[a]

$$p_{ji}=-[(i-s)^2(x/c)(r/a)+\Sigma R_{jk}(r)\sin(\lambda_{jk}x/c)](c/a)\hat{K}$$

$$u_{ji}=-[(i-s)(r/a)+(i-s)^{-1}\Sigma R_{jk}\lambda_k\cos(\lambda_{jk}x/c)]\hat{K}$$

$$v_{ji}=[(i-s)^2(i-s)^{-1}(x/c)+\Sigma R_{vjk}\sin(\lambda_{jk}x/c)](c/a)\hat{K}$$

$$w_{ji}=[-i(i-s)^2(i+s)^{-1}(x/c)+\Sigma R_{wjk}\sin(\lambda_{jk}x/c)](c/a)\hat{K}$$

$$R_{jk}=E_{jk}J_1(\hat{r})+F_{jk}Y_1(\hat{r})$$

$$R_{vjk}=[(s-i)aR'_{jk}-2i(a/r)R_{jk}]S^{-1}$$

$$R_{wjk}=-[2aR'_{jk}+i(s-i)(a/r)R_{jk}]S^{-1}$$

$$\hat{r}=\hat{\lambda}_{jk}r/c$$

$$\hat{\lambda}^2_{jk}=-\left[\frac{S}{(s-i)^2}\right]\lambda^2_{jk}$$

$S=s^2-2is+3$; and J_1 and Y_1 are Bessel functions of order one of the first and second kinds, respectively.

[a]The conditions for the E_{jk}'s and F_{jk}'s are given in Sec. V. Note that the definitions of E_{jk} and F_{jk} in R_{jk} differ from those of E_k and F_k in Ref. 3.

The differential equations for the inviscid functions of each liquid are the same as those for a single liquid and the solutions have the same form.[3]

More specifically, the pressure and velocity perturbations are expressed as the sum of products of functions of x and r. The functions of x are 1, x/a, $\sin(\lambda_{jk}x/a)$, and $\cos(\lambda_{jk}x/a)$, where

$$\lambda_{jk}=(\pi k/2)[1+\delta_{cj}]; \qquad k=1,3,5\ldots(2N_k-1) \quad (26)$$

$$\delta_{cj}=\frac{-(a/c)(1+i)}{2\sqrt{2}(1+is)}\left\{\frac{1-is}{\sqrt{3+is}}+\frac{i(3+is)}{\sqrt{1-is}}\right\}Re_j^{-1/2} \quad (27)$$

$$\mathrm{Re}_j=\frac{a^2\dot{\phi}}{\nu_j} \quad (28)$$

The specific expressions for pressure and velocity functions are given in Table 1.

IV. The Viscous Solution

In Ref. 3, the viscous parts of the perturbation variables were important only in a small region near the cylinder wall and the endwalls, and these functions were computed by the use of unsteady boundary layer equations in these regions. It is reasonable to expect that the viscous parts can also have contributions near the liquid interface and that derivatives in the radial direction are much larger than those in the circumferential or axial directions. Thus, we will assume that the viscous functions away from the endwalls satisfy the same equations as those for the cylindrical wall boundary layers.[3]

$$(s-i)w_{jv}=a^2Re_j^{-1}\frac{\partial^2 w_{jv}}{\partial r^2} \quad (29)$$

$$(s-i)u_{jv}=a^2Re_j^{-1}\frac{\partial^2 u_{jv}}{\partial r^2} \quad (30)$$

$$a\frac{\partial p_{jv}}{\partial r}=2w_{jv} \quad (31)$$

$$\frac{\partial(rv_{jv})}{\partial r}=iw_{jv}-r\frac{\partial u_{jv}}{\partial x} \quad (32)$$

The solutions to Eqs. (29-31) are

$$(w_{1v},u_{1v},p_{1v})=(w_{10},u_{10},2\delta_{a1}w_{10})e^{(r-a)/a\delta_{a1}}+(w_{11},u_{11},-2\delta_{a1}w_{11})e^{-(r-b_1)/a\delta_{a1}} \quad (33)$$

$$(w_{2v},u_{2v},p_{2v})=(w_{21},u_{21},2\delta_{a2}w_{21})e^{(r-b_1)/a\delta_{a2}}+(w_{22},u_{22},-2\delta_{a2}w_{22})e^{-(r-b_1)/a\delta_{a2}} \quad (34)$$

where

$$\delta_{aj}=\frac{1+i}{\sqrt{2(1+is)}}Re_j^{-1/2}$$

and the eight coefficients u_{jk}, w_{jk} are functions of x. Four conditions on the coefficients come from the continuity of tangential velocities and shears [Eqs. (17) and (18)] at the interface

$$\Delta w_i+w_{10}\epsilon_1+w_{11}-w_{21}-w_{22}\epsilon_2=0 \quad (35)$$

$$\Delta u_i+u_{10}\epsilon_1+u_{11}-u_{21}-u_{22}\epsilon_2=0 \quad (36)$$

$$w_{10}\epsilon_1-w_{11}=N(w_{21}-w_{22}\epsilon_2) \quad (37)$$

$$u_{10}\epsilon_1-u_{11}=N(u_{21}-u_{22}\epsilon_2) \quad (38)$$

where

$$\Delta w_i = [w_{1i} - w_{2i}]_{r=b_1}$$

$$\Delta u_i = [u_{1i} - u_{2i}]_{r=b_1}$$

$$\epsilon_1 = \exp[(b_1 - a)/a\delta_{a1}]$$

$$\epsilon_2 = \exp[(b_2 - b_1)/a\delta_{a2}]$$

$$N = \rho_{21}\sqrt{\nu_2/\nu_1}$$

Four more conditions come from the no-slip condition at the cylindrical wall [Eqs. (19) and (21)] and the no-shear condition of the free surface [Eqs. (23-24)]:

$$w_{1i}(a,x) + w_{10} + w_{11}\epsilon_1 = i(s-i)\hat{K}(x/a) \tag{39}$$

$$u_{1i}(a,x) + u_{10} + u_{11}\epsilon_1 = (s-i)\hat{K} \tag{40}$$

$$w_{21}\epsilon_2 - w_{22} = 0 \tag{41}$$

$$u_{21}\epsilon_2 - u_{22} = 0 \tag{42}$$

Equations (35-42) can now be used to determine the eight coefficient functions. If the total liquid occupies an annular region that is thicker than ten boundary layer thicknesses, the product $\epsilon_1\,\epsilon_2$ is quite small and can be neglected. The resulting expressions for the coefficient functions are given in Table 2. If the liquid interface is more than ten boundary layer thicknesses from both the cylindrical surface and the free surface, both ϵ_1 and ϵ_2 are very small and can be disregarded in Table 2.

The third component of Eqs. (33-34) can be used in conjunction with Eqs. (37) and (41) to yield general relations for the viscous perturbation pressures at the three boundaries:

$$p_{1v}(a/x) = 2\delta_{a1}(w_{10} - w_{11}\epsilon_1) \tag{43}$$

$$p_{1v}(b_1,x) = \rho_{21}p_{2v}(b_1,x) \tag{44}$$

$$p_{2v}(b_2,x) = 0 \tag{45}$$

In order to compute the viscous radial velocity, we must use an inequality involving the magnitude of a complex exponential:

$$\left|\frac{\Delta r}{a}\exp\left\{-\frac{\Delta r}{a\delta_{aj}}\right\}\right| = \left|\frac{\Delta r}{a}\exp\left\{-\frac{\Delta r d_R}{a|\delta_{aj}|^2}\right\}\right|$$

$$\leq \frac{|\delta_{aj}|^2}{d_R e} \leq |\delta_{aj}| \quad \text{for} \quad \epsilon < |\tau^{-1} - 1|/10 \tag{46}$$

where

$$\delta_{aj} = d_R + id_I,\ d_R > 0,\ |d_I| \doteq |d_R|\left|1 - \frac{\epsilon\tau}{1-\tau}\right|,\ \Delta r > 0$$

The first two components of Eqs. (33-34) can now be substituted in Eq. (32), which can now be integrated to find v_{jv}. Simplification by use of inequality (46) and neglecting $|\delta_{aj}|^2$ terms yields:

$$rv_{1v} = a\delta_{a1}\{v_{10}e\exp[(r-a)/a\delta_{a1}] + v_{11}e\exp[-(r-b_1)/a\delta_{a1}]\} \tag{47}$$

$$rv_{2v} = a\delta_{a2}\{v_{21}e\exp[(r-b_1)/a\delta_{a2}] + v_{22}e\exp[-(r-b_2)/a\delta_{a2}]\} \tag{48}$$

where $v_{10} = iw_{10} - au'_{10}$, $v_{11} = -[iw_{11} - b_1u'_{11}]$, $v_{21} = iw_{21} - b_1u'_{21}$, and $v_{22} = -[iw_{22} - b_2u'_{22}]$.

Equations (47-48) can now be used in conjunction with Eqs. (37), (38), (41), and (42) to give relations for the radial viscous velocity at the three boundaries:

$$v_{1v}(a,x) = [v_{10} + v_{11}\epsilon_1]\delta_{a1} \tag{49}$$

$$v_{1v}(b_1,x) = \rho_{21}v_{2v}(b_1,x) = \rho_{21}[v_{21} + \epsilon_2 v_{22}](a/b_1)\delta_{a2} \tag{50}$$

$$v_{2v}(b_2,x) = 0 \tag{51}$$

where v_{jk} are given in Table 2 [Eq. (46) was used to simplify entries in this Table].

V. Inviscid Boundary Conditions

In the previous section we used eight of the twelve liquid boundary conditions to determine the viscous perturbations in terms of the inviscid perturbations. We will now completely determine the inviscid perturbation by use of the remaining four conditions—Eqs. (16), (20) and (22), and $v_{1s} = v_{2s}$ at the interface. These conditions can be simply stated using Eqs. (44), (45), (50), and (51):

at $r = a$

$$v_{1i} + v_{1v} = (i-s)(x/a)\hat{K} \tag{52}$$

at $r = b_1$

$$p_{1i} + \frac{b_1 v_{1i}}{a(s-i)} = \rho_{21}\left[p_{2i} + \frac{b_1 v_{2i}}{a(s-i)}\right] \tag{53}$$

Table 2 Viscous coefficient functions for internal free surface

$$w_{10} = \{[1 + N + (1-N)\epsilon_2^2]w_a + N\epsilon_1\Delta w_{si}\}D^{-1}$$

$$w_{11} = \{(1-N)\epsilon_1 w_a - N(1-\epsilon_2^2)\Delta w_{si}\}D^{-1}$$

$$w_{21} = \{2\epsilon_1 w_a + (1+\epsilon_1^2)\Delta w_{si}\}D^{-1}$$

$$w_{22} = \epsilon_2\Delta w_{si}D^{-1}$$

$$u_{10} = \{[1 + N + (1-N)\epsilon_2^2]u_a + N\epsilon_1\Delta u_{si}\}D^{-1}$$

$$u_{11} = \{(1-N)\epsilon_1 u_a - N(1-\epsilon_2^2)\Delta u_{si}\}D^{-1}$$

$$u_{21} = \{2\epsilon_1 u_a + (1+\epsilon_1^2)\Delta u_{si}\}D^{-1}$$

$$u_{22} = \epsilon_2\Delta u_{si}D^{-1}$$

$$v_{10} = \{[1 + N + (1-N)\epsilon_2^2]v_a + N\epsilon_1\Delta^*\}D^{-1}$$

$$v_{11} = \{-(1-N)\epsilon_1 v_a + N(1-\epsilon_2^2)\Delta^*\}D^{-1}$$

$$v_{21} = \{2\epsilon_1 v_a + (1+\epsilon_1^2)\Delta^*\}D^{-1}$$

$$v_{22} = -\epsilon_2\Delta^* D^{-1}$$

where

$$w_a = i(s-i)(x/a)\hat{K} - w_{1i}(a,x)$$

$$u_a = (s-i)\hat{K} - u_{1i}(a,x)$$

$$v_a = (s-i)(x/a)\hat{K} - \left[\frac{\partial(rv_{1i})}{\partial r}\right]_{r=a}$$

$$D = 1 + N + (1-N)(\epsilon_1^2 + \epsilon_2^2)$$

$$\Delta^* = \left[\frac{\partial(rv_{1i})}{\partial r} - \frac{\partial(rv_{2i})}{\partial r}\right]_{r=b_1}$$

$$v_{1i} = v_{2i} + (1-\rho_{21})v_{2v} \tag{54}$$

and at $r = b_2$

$$p_{2i} + \frac{b_2 v_{2i}}{a(s-i)} = 0 \tag{55}$$

Equations (52-55), with v_{1v} and v_{2v} set equal to zero, were used by Scott[9] to obtain eigenfrequencies for a completely inviscid liquid payload. As can be seen from Table 1, for each k, four constants must be established to completely determine the inviscid perturbation functions, i.e., E_{1k}, E_{2k}, F_{1k}, and F_{2k}. [For the special case of 100% filled cylinder ($b_2 = 0$), F_{2k} is zero and, instead of $4N_k$ constants, only $3N_k$ constants remain to be determined.

When the expansions for the inviscid pressures and velocities in Table 1 are inserted in Eqs. (52-55), four equations in $4N_k$ unknowns are obtained in the following format:

$$F_j = b_j(x) \qquad j = 1,2,3,4 \tag{56}$$

where

$$F_j = \Sigma E_{1k} A_{kj}(x) + \Sigma E_{2k} B_{kj}(x) + \Sigma F_{1k} C_{kj}(x) + \Sigma F_{2k} D_{kj}(x)$$

If R^2 is defined as

$$R^2 = \sum_{j=1}^{4} (F_j - b_j)^2 \tag{57}$$

the least squares fit conditions can be derived in the usual way. In calculations of this paper, N_k was 9 and a 36×36 matrix had to be inverted to determine the 36 parameters in Eq. (56). If $\nu_1 = \nu_2$ and $\lambda_{1k} = \lambda_{2k}$, the one large matrix inversion can be replaced by inversions of nine 4×4 matrices.†

VI. Liquid Moment

For coning motion described by Eq. (1), the linear liquid pitch and yaw moment is defined to be[3]

$$M_{L\tilde{Y}} + iM_{L\tilde{Z}} = m_L a^2 \dot{\phi}^2 \tau (C_{\mathrm{LSM}} + iC_{\mathrm{LIM}}) \hat{K} e^{is\phi} \tag{58}$$

where $m_L = 2\pi\rho_1 a^2 c$.

The major components of this liquid moment are due to the pressure on the lateral wall and endwalls of the container. Lesser components result from the viscous wall shear on the lateral wall and endwalls. Thus, the liquid moment coefficient can be given as a sum of four terms. (For simplicity, these terms will be computed for the center of the cylinder at the center of mass of the projectile. More complete expressions are given in Ref. 3.)

$$\tau(C_{\mathrm{LSM}} + iC_{\mathrm{LIM}}) = m_{p\ell} + m_{pe} + m_{v\ell} + m_{ve} \tag{59}$$

By using Eqs. (2-4) and (10), the linear periodic part of the pressure can be computed in cylinder-fixed coordinates

$$\frac{\Delta P}{\rho_1 a^2 \dot{\phi}^2} = \mathrm{Re}\{[\tilde{p}_{1i}(\tilde{r},\tilde{x})] e^{s\phi - i\tilde{\theta}}\} \qquad \text{for } b_1 < \tilde{r} < a$$
$$= \rho_{21} \mathrm{Re}\{[\tilde{p}_{2i}(\tilde{r},\tilde{x})] e^{s\phi - i\tilde{\theta}}\} \qquad \text{for } b_2 < \tilde{r} < b_1 \tag{60}$$

where $\tilde{p}_{ji}(\tilde{r},\tilde{x}) = p_{ji}(\tilde{r},\tilde{x}) - (\tilde{r}\tilde{x}/a^2)\hat{K}$.

The inviscid pressure [Eq. (60)] and the viscous lateral wall pressure caused by the centripetal terms in the boundary layer [Eq. (43)] can be integrated to yield the pressure moment coefficient on the lateral wall.

$$m_{p\ell} = i(2ac\hat{K})^{-1} \int_{-c}^{c} \tilde{x}[\tilde{p}_{1i}(a,\tilde{x}) + p_{1v}(a,\tilde{x})]\, d\tilde{x} \tag{61}$$

where $p_{1v}(a,\tilde{x}) = 2\delta a 1(w_{10} - w_{11}\epsilon_1)$.

Since the viscous pressure on the endwalls is zero, the expression for the pressure moment coefficient on the endwalls is slightly simpler:

$$m_{pe} = -i(a^2 c\hat{K})^{-1} \left\{ \int_{b_1}^{a} \tilde{p}_{1i}(\tilde{r},c)\tilde{r}^2 d\tilde{r} + \rho_{21} \int_{b_2}^{b_1} \tilde{p}_{2i}(\tilde{r},c)\tilde{r}^2 d\tilde{r} \right\} \tag{62}$$

The visocus moment coefficient on the lateral wall can be computed by using Eq. (33).

$$m_{v\ell} = (2ac\hat{K}Re_1\delta_{a1})^{-1} \int_{-c}^{c} [ia(u_{10} - \epsilon_1 u_{11}) + \tilde{x}(w_{10} - \epsilon_1 w_{11})]\, d\tilde{x} \tag{63}$$

The viscous moment coefficient on the endwalls is a little more difficult to compute since a change in kinematic viscosity, as well as a change in density, can occur across the interface. The relations of Ref. 3 can, however, be used to obtain the following result:

$$m_{ve} = \left(\frac{\sqrt{i+s}}{a^2\hat{K}}\right) Re_1^{-1/2} \left[\int_{b_1}^{a} w_1(\tilde{r})\tilde{r}\, d\tilde{r} + N \int_{b_2}^{b_1} w_2(\tilde{r})\tilde{r}\, d\tilde{r} \right] \tag{64}$$

where $w_j(\tilde{r}) = 2(1+is)(c/a)\,\hat{K} - w_{ji}(\tilde{r},c) + iv_{ji}(\tilde{r},c)$.

VII. Discussion

For specified s, the least squares fit of Eqs. (52-55) yields values of E_{1k}, E_{2k}, F_{1k}, and F_{2k} for $k = 1,3\ldots, N_k$. These values in turn determine the k component of the liquid moment. Values of s that make the k component infinitely large are called eigenvalues, s_{kn}, where k is the axial mode number and n is the radial mode number. The imaginary parts of the s_{kn}'s are eigenfrequencies, τ_{kn}, of the transient motion in the liquid, and the real parts are the damping rates of that motion. When the forced coning motion of the projectile has a frequency near one of the above eigenfrequencies, the liquid side moment has a local maximum. For this reason, the eigenfrequencies are of considerable interest to a projectile designer. The equations of this paper have been coded for the VAX 11/780 computer, and eigenfrequencies can be computed for specified values of c/a, Re, k, ρ_{21}, N, b_1/a, and b_2/a.

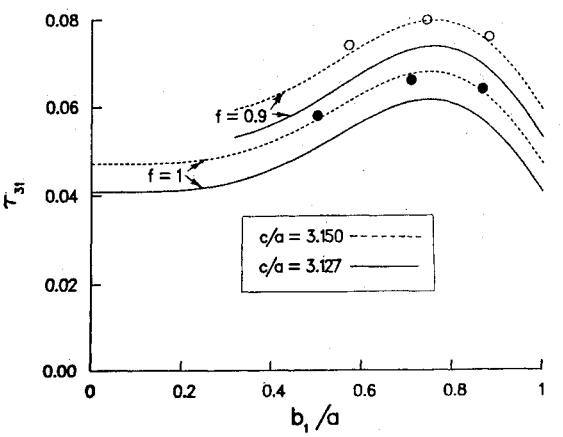

Fig. 1 τ_{31} vs b_1/a for $Re_1 = 2 \times 10^6$, $c/a = 3.127$, $\rho_{21} = .82$, $\nu_1 = \nu_2$, and various free surface fill ratios (experimental data are from Ref. 9).

†All the calculations presented in this paper are for this simple case. A computer code for $\nu_1 \neq \nu_2$ is available for the VAX and some results are given in Ref. 10.

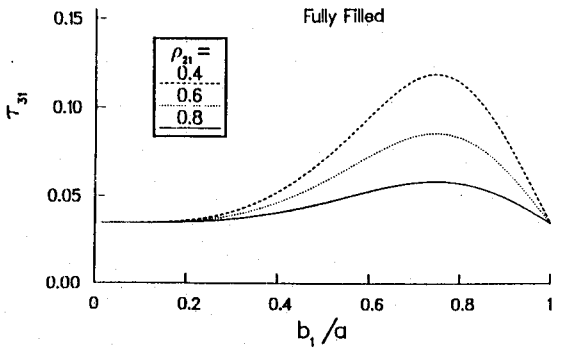

Fig. 2 τ_{31} vs b_1/a for $Re_1 = 4\times10^4$, $c/a = 3.1$, $f = 1$, $\nu_1 = \nu_2$, and various density ratios.

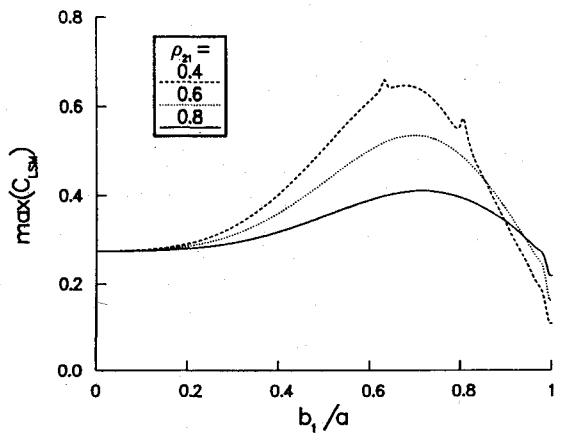

Fig. 3 τ_{31} maximum side moment coefficient vs b_1/a for $Re_1 = 4\times10^4$, $c/a = 3.1$, $f = 1$, $\nu_1 = \nu_2$, and various density ratios.

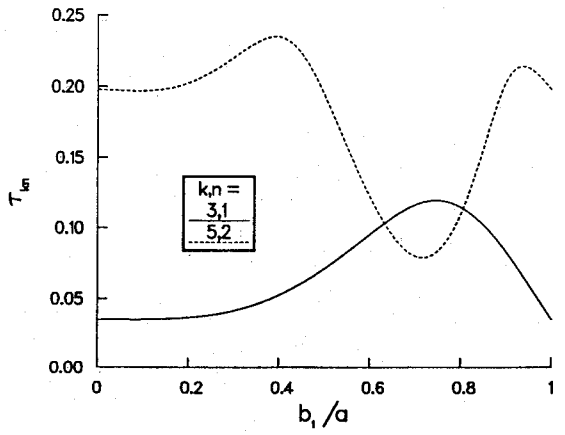

Fig. 4 τ_{31} and τ_{52} vs b_1/a for $Re_1 = 4\times10^4$, $c/a = 3.1$, $f = 1$, $\rho_{21} = .4$, $\nu_1 = \nu_2$.

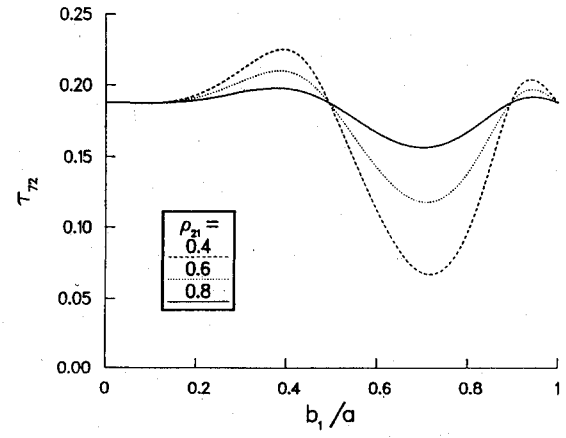

Fig. 5 τ_{72} vs b_1/a for $Re_1 = 10^6$, $c/a = 4.29$, $f = 1$, $\nu_1 = \nu_2$, and various density ratios.

Scott's experimental data were for $c/a = 3.127$, $Re_1 = 2\times10^6$, $\rho_{21} = .82$, $\nu_2 = \nu_1$, and $f = 0.9$, 1. (The second, third, and fourth columns of Scott's Table 1 are mislabeled in Ref. 9. In his notation, they should be identified as d/c, bdc^{-2}, and adc^{-2}.) In Fig. 1, his data are compared with the theory of this paper and we see that the maximum error is 14%. In Ref. 3 it was found that much better fits could be obtained by using a slightly different value of the fineness ratio. Indeed, effective fineness ratio values that were 0.5% greater than the measured value would provide excellent agreement with the data of that paper. In Fig. 1 it is shown that a 0.7% greater fineness ratio ($c/a = 3.150$) gives excellent agreement for six different experiments.

In Figs. 2 and 4-6, computed eigenfrequencies for a completely filled cylinder ($b_2 = 0$) are plotted as functions of b_1/a over the range zero to one. For zero, the cylinder is filled with the heavier liquid, and for unity, it is filled with the lighter liquid. Since the single-liquid eigenfrequency is not a function of density, the eigenfrequency at the two extremes of b_1/a should equal the value predicted by the Stewartson-Wedemeyer theory. In all cases computed, this is found to be true.

An important characterisic of an eigenfrequency is the occurrence of a maximum side moment coefficient for a coning motion with constant damping and a frequency near the eigenfrequency. The theory of this paper was used to compute the maximum side moment coefficients for the conditions of Fig. 2, and the constant amplitude coning motion with frequency near τ_{31}. The resulting curves are given in Fig. 3, and have a number of interesting properties.

As b_1/a varies from 0 to 1, the heavier liquid is replaced by the lighter liquid. Since the side moment is defined in terms of the density ρ_1 of the heavier liquid, a requirement for our C_{LSM} (b_1/a) is that

$$C_{LSM}(1) = \rho_{21} C_{LSM}(0) \tag{65}$$

This requirement was satisfied by our calculations. It is important to note that as b_1/a goes to 1 in the region $b_1/a < 1 - 3\,|\delta_{a1}|$, the apparent limit value of the liquid side moment coefficient is quite different from its value at the wall. Thus, a small amount of the heavier fluid can have a very noticeable effect on the side moment.

When b_1/a is quite close to unity, the free boundary layer associated with the interface merges with the lateral wall boundary layer to form a boundary region. As long as the derivatives normal to the wall are much greater than the derivatives along the wall, the solution given by this paper should be valid. Even if this boundary region is improperly computed, it would affect only the details of its variation with amount of impurity; it would not affect the large change in C_{LSM} caused by a small impurity.

An interesting feature of the $\rho_{21} = .4$ side moment coefficient curve is the presence of two small peaks. It seems likely that this is caused by the equality of τ_{31} and τ_{52} at these locations of the interface. Figure 4 compares the dependence of τ_{52} on interface location with that of τ_{31} for $\rho_{21} = .4$. For $n = 1$, the eigenfrequency has one maximum, while for $n = 2$, the corresponding eigenfrequency has two maxima; for this density ratio, those eigenfequency curves do intersect. Since the real parts of the corresponding eigenvalues are not equal, the eigenvalues are not equal even when the eigenfrequencies are the same.

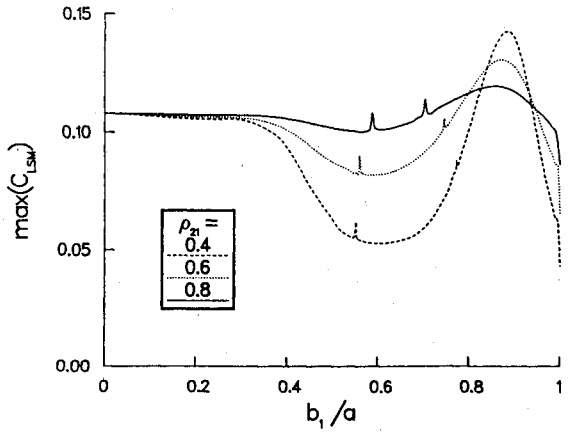

Fig. 6 τ_{72} maximum side moment coefficient vs b_1/a for $Re_1 = 10^6$, $c/a = 4.29$, $f = 1$, $\nu_1 = \nu_2$, and various density ratios.

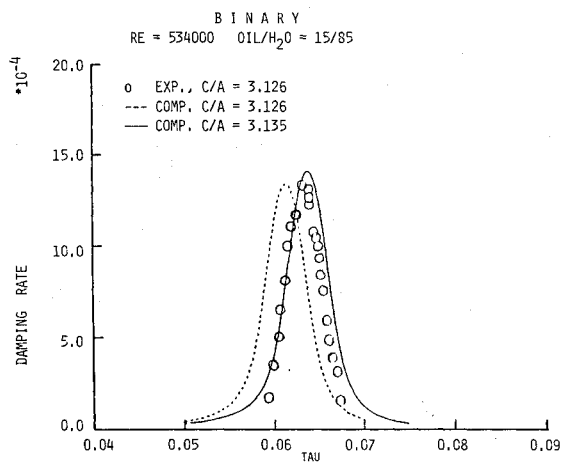

Fig. 7 Damping rate, $-\epsilon\tau$, vs τ for $Re_1 = 5.34 \times 10^5$, $f = .89$, $\rho_{21} = 0.812$, $\nu_1 = \nu_2$.

The coalescence of eigenfrequencies for special interface locations also occurs for the fineness ratio of 4.29, extensively studied by D'Amico and Miller.[11-13] For this case, the primary eigenfrequency of interest is τ_{72} and is plotted in Fig. 5 for three density ratios. This eigenfrequency has two maxima (since $n = 2$), and it has the single-liquid value for $b_1/a = 0$, 0.49, 0.89, 1.0 for all density ratios. In Fig 6, the τ_{72} maximum side moment coefficient is plotted against b_1/a for three density ratios; all three curves show the presence of an eigenfrequency coalescence (the other eigenfrequency is $\tau_{11,3}$).

Measurements of gyroscope damping rate produced by a mixture of oil and water have recently been made by Kayser et al.[14] For a mixture of 15% silicon oil and 85% water, this damping rate is plotted against τ in Fig. 7. This mixture occupied 89% of a cylindrical container mounted in the gyroscope. The theoretical side moment can be used to predict the damping rate. This prediction is shown as the dashed curve. The shape of the curve is good, but there is a frequency bias of 0.0025. This bias corresponds to changing the fineness ratio 0.3% from the actual value of 3.126 to an effective value of 3.135. (This purely empirical effect of a small *repeatable* increase in fineness ratio has been observed frequently and efforts to find a theoretical basis are continuing.)

VIII. Conclusions

The linear boundary layer theory for the response of a liquid payload to spinning and coning motions has been extended to the case of two liquids. With the exception of an unexplained frequency bias, this theory predicts eigenfrequencies and side moments which agree very well with the results of experiments. For certain locations of the liquid interface, the theory shows that pairs of eigenfrequencies can coalesce. The theory also predicts a significant change in side moment caused by the presence of a small amount of heavier liquid.

Acknowledgment

The author is deeply indebted to Mr. James W. Bradley for checking most of the equations of this paper and coding all the calculations on the VAX 11/780 computer. The correct equations and calculations are the result of Mr. Bradley's very capable efforts while any errors are blunders on the author's part.

References

[1]Stewartson, K., "On the Stability of a Spinning Top Containing Liquid," *Journal of Fluid Mechanics,* Vol. 5, Part 4, Sept. 1959, pp. 577-592.

[2]Wedemeyer, E.H., "Viscous Correction to Stewartson's Stability Criterion," ARBRL-MR-1325, Ballistic Research Laboratory, Aberdeen Proving Ground, MD, June 1966.

[3]Murphy, C.H., "Angular Motion of a Spinning Projectile with a Viscous Liquid Payload," ARBRL-MR-03194, Ballistic Research Laboratory, Aberdeen Proving Ground, MD, Aug. 1982. (See also *Journal of Guidance, Control, and Dynamics,* Vol. 6, July-Aug. 1983, pp. 280-286.)

[4]Kitchens, C.W. Jr., Gerber, N., and Sedney, R., "Oscillations of a Liquid in a Rotating Cylinder: Solid Body Rotation," ARBRL-TR-02081, Ballistic Research Laboratory, Aberdeen Proving Ground, MD, June 1978.

[5]Gerber, N., Sedney, R., and Bartos, J.M., "Pressure Moment on a Liquid-Filled Projectile: Solid Body Rotation," ARBRL-TR-02422, Ballistic Research Laboratory, Aberdeen Proving Ground, MD, Oct. 1982.

[6]Gerber, N., and Sedney, R., "Moment on a Liquid-Filled Spinning and Nutating Projectile: Solid Body Rotation," ARBRL-TR-02470, Ballistic Research Laboratory, Aberdeen Proving Ground, MD, 1983.

[7]Murphy, C.H., "Liquid Payload Roll Moment Induced by a Spinning and Coning Projectile," ARBRL-TR-02521, Ballistic Research Laboratory, Aberdeen Proving Ground, MD, Sept. 1983. (See also AIAA Paper 83-2142, Aug. 1983.)

[8]Murphy, C.H., "A Relation Between Liquid Roll Moment and Liquid Side Moment," *Journal of Guidance and Control,* Vol. 8, March-April 1985, pp. 287-288.

[9]Scott, W.E., "The Inertial Wave Frequency Spectrum in a Cylindrically Confined, Inviscid, Incompressible Two Component Liquid," ARBRL-MR-1609, Ballistic Research Laboratory, Aberdeen Proving Ground, MD, Sept. 1972, (See also *Physics of Fluids,* Vol. 16, No. 1, Jan. 1973, pp. 9-12.

[10]Murphy, C.H., "Side Moment Exerted by a Two-Component Liquid Payload on a Spinning Projectile," ARBRL-TR-2624, Ballistic Research Laboratory, Aberdeen Proving Ground, MD, Dec. 1984.

[11]Miller, M.C., "Flight Instabilities of Spinning Projectiles Having Nonrigid Payloads," *Journal of Guidance, Control, and Dynamics,* Vol. 5, March-April 1982, pp. 151-157.

[12]D'Amico, W.P. and Miller, M.C., "Flight Instability Produced by a Rapidly Spinning, Highly Viscous Liquid," *Journal of Spacecraft and Rockets,* Vol. 16, Jan.-Feb. 1979, pp. 62-64.

[13]D'Amico, W.P., and Clay, W.H., "High Viscosity Liquid Payload Yawsonde Data for Small Launch Yaws," ARBRL-MR-03029, Ballistic Research Laboratory, Aberdeen Proving Ground, MD, June 1980.

[14]Kayser, L.D., D'Amico, W.P., and Brannan, W.I., "Free Gyroscope Experiments of Two Immiscible Liquids in a Partially Filled Container," ARBRL-MR-3484, Ballistic Research Laboratory, Aberdeen Proving Ground, MD, Dec. 1985. (See also AIAA Paper 85-1823, Aug. 1985.)